Root branching in salt requires auxin-independent modulation of LBD16 function

Yanxia Zhang[1,2,3*], Yiyun Li[1], Thijs de Zeeuw[1], Kilian Duijts[1], Dorota Kawa[2,a], Jasper Lamers[1], Kristina S. Munzert[4], Hongfei Li[1], Yutao Zou[1], A. Jessica Meyer[1], Jinxuan Yan[1], Francel Verstappen[1], Yixuan Wang[1], Tom Gijsberts[1], Jielin Wang[1], Nora Gigli-Bisceglia[1,b], Timo Engelsdorf[4], Aalt D.J van Dijk[5] and Christa Testerink[1*]

1 Laboratory of Plant Physiology, Wageningen University & Research, The Netherlands

2 Plant Cell Biology, Faculty of Science, Swammerdam Institute for Life Sciences, University of Amsterdam, The Netherlands

3 College of Agriculture, South China Agricultural University, China

4 Molecular Plant Physiology, Philipps-Universität Marburg, Germany

5 Bioinformatics Group, Wageningen University & Research, The Netherlands

*Corresponding authors: yanxia.zhang@scau.edu.cn, Christa.Testerink@wur.nl

a present address: Department of Plant Biology and Genome Centre, University of California, Davis, California

b present address: Plant Stress Resilience, Utrecht University

Abstract

Salinity stress constrains lateral root (LR) growth and severely impacts plant growth. Auxin signaling is indispensable for the regulation of LR formation. Nevertheless, the molecular mechanism of how salinity affects root auxin signaling and whether salt would steer alternative pathway(s) to regulate LR development is unknown. Here we show that the auxin-regulated transcription factor LATERAL ORGAN BOUNDARY DOMAIN (LBD)16, known as an essential player for LR development under control conditions, is regulated by an alternative non-canonical pathway under salinity. Salt represses auxin signaling but in parallel activates an upstream transcriptional activator of LBD16, ZINC FINGER OF ARABIDOPSIS THALIANA 6 (ZAT6). ZAT6 modulates the activity of *LBD16* to contribute to downstream cell wall remodeling, and promotes LR development under salinity stress. Our study thus shows that root developmental plasticity in response to salt stress is achieved by integration of auxin-dependent repressive and salt-activated auxin-independent pathways converging on LBD16 to modulate root branching modulation under salinity.

Key Words

auxin, cell wall remodeling, lateral root development, *LBD16*, salinity stress

Introduction

Plant root system architecture (RSA) acclimation is important for plants' survival and productivity in response to environmental challenges. In Arabidopsis, lateral roots (LRs) contribute the majority of the mature root system architecture. Their formation and growth are tightly regulated by both internal chemical signals and external environmental cues, for example soil salinity and water availability[1,2]. LRs are specified within the main root oscillation zone - from the basal meristem zone through the elongation zone- and initiated from xylem pole pericycle (XPP) cells in the differentiation zone[3,4]. During LR initiation, asymmetric cell division takes place and results in the formation of Stage I lateral root primordia (LRP) in the early differentiation zone, which is followed by early morphogenesis (Stage II through IV) and further meristem organization (Stage V to VIII) of the LRP to traverse the overlaying cell layers and establish emerged LRs[3-5]. Cell wall changes have been observed to occur in the LRP overlaying endodermal cell layer of maize plants as early as in the 1970s[6]. Recently, pectin esterification state at LR initiation sites, as a result of the action of several pectin methylesterases (PMEs) (PME2, 3 and 5) and PME inhibitor 3 (PMEI3), was reported to affect LR formation in Arabidopsis[7]. Additionally, the cell wall-loosening proteins - EXPANSIN (EXP) A1, 14 and 17 - were also reported to promote LR formation[8-10]. Thus, LR development requires coordination of cell division and cell wall modifications to accommodate the emerging LRs.

The plant hormone auxin plays indispensable roles during various stages of LRP development from initiation to LR emergence via different AUXIN RESPONSE FACTOR (ARFs)-mediated transcriptional modules[11,12]. Arabidopsis ARF7 and ARF19 were shown to mediate LR development by transcriptional regulation of several redundant LATERAL ORGAN BOUNDARY DOMAIN (LBD)-type transcription factors including LBD16, LBD18, LBD29 and LBD33 to mediate LR development[13-15]. Auxin was shown to be upstream of the cell wall remodeling pathway(s) during LR development. For example, auxin induces IDA-HAE/HSL2 ligand-receptor signaling to active a MAPK cascade MKK4/MKK5–MPK3/MPK6 which is required to for the expression of cell wall remodeling genes during LR emergence[16,17]. The enzymes xyloglucan endotransglucosylases (XTH) 9 and 23, involved in the endotransglucosylation and endohydrolysis of the major cell wall hemicellulose xyloglucan, were shown to act downstream of auxin signaling mediating LR development[16,18]. In summary, auxin, cell wall modification and their interplays are all playing essential roles in mediating LR development. However, it is not clear how auxin signaling and cell wall

71 modifications during LR development are modulated in response to external environmental
72 signals.

73 In response to salinity stress, Arabidopsis plants remodel their RSA through modulation
74 of LR emergence and elongation[1,19-21], resulting in shorter, fewer LRs in general, although
75 natural variation in the response has been found. Several novel genetic components
76 contributing to the LR developmental plasticity in response to salinity in Arabidopsis have been
77 identified, including *High-affinity K^+ transporter 1* (*HKT1*) and *CYTOCHROME P450*
78 *FAMILY 79 SUBFAMILY B2* (*CYP79B2*)[1], coding for proteins involved in Na^+/K^+ homeostasis
79 and auxin-related metabolite biosynthesis, respectively. Nevertheless, these studies cannot
80 explain how auxin signals are affected during LR development in salt, and how salt impacts
81 the core LR developmental pathways is largely unknown.

82 Here we report that LBD16 is a crucial mediator of LR developmental plasticity in salt,
83 enabling cell wall remodeling. We show that salt upregulates *LBD16* expression in the main
84 root zones and developing LRP independently of ARF7/19. Simultaneously, we observe a
85 reduction in root auxin levels upon salt stress, revealing the presence of an alternative auxin-
86 independent pathway promoting LBD16 upregulation by salt stress. Yeast-one-hybrid
87 screening combined with transcriptomic analysis and network inference identified additional
88 potential salt stress-induced upstream transcriptional regulators of LBD16. We predicted the
89 C2H2-type transcription factor ZINC FINGER OF ARABIDOPSIS THALIANA 6 (ZAT6), to
90 play a pivotal role in activating *LBD16* in response to salinity and could indeed confirm that
91 ZAT6 binds to the promoter of *LBD16*, acting independent from ARF7/19 to positively regulate
92 *LBD16* expression, contributing to cell wall modifications in roots in response to salinity. Loss-
93 of-function mutants of *ZAT6* displayed salt stress-induced defects in LR development and cell
94 wall composition, similar to the *lbd16-1* mutants. Our study thus provides molecular insights
95 into the coordination of LR developmental plasticity mediated by a salt-activated pathway that
96 positively impacts root branching.

97

98 **Results**

99 ***LBD16* is a central regulator of the plasticity of LR development in response to salinity**

100 RSA analyses of the Arabidopsis HapMap natural diversity panel in response to salt
101 stress have identified the previously identified the auxin-dependent transcription factor LBD16
102 as a candidate locus regulating RSA remodeling in response to salt stress[1]. Since LBD16 had

103 been already known to regulate LR development[13,14], we further characterized the RSA of
104 knock-out and complementation lines of *LBD16* under control and salt conditions. We found
105 that the decrease in emerged LR density of two independent *lbd16* mutants in response to salt
106 was more severe compared to the wild type Col-0 (**Fig. 1a, b, Fig.S1**). This reduced LR density
107 was not due to main root length differences between Col-0 and the mutants and a genomic
108 region of *LBD16* gene was able to restore the profound decrease in emerged LR density in the
109 *lbd16-1* mutant under both mild (75 mM NaCl) and severe (125 mM NaCl) salt stress
110 conditions (**Fig. S2**). No significant decrease was found in LR density under control conditions
111 in the *lbd16* knock-out mutants compared to Col-0 (**Fig. 1a, b and Fig. S2a, b**), which is in
112 agreement with previous reports showing a functional redundancy of LBD16 with LBD18 and
113 LBD33 under optimal conditions with regard to LR development[13,22].

114 To further understand how *LBD16* may act under saline conditions, we investigated
115 microscopic LRP development in Col-0 and *lbd16-1* in response to mild and severe salt stress.
116 In line with the reported effect of *lbd16* mutant on LR density[13], we also observed a lower
117 density of non-emerged LRP (Stage I through VII) in *lbd16-1* than in Col-0 under control
118 condition (**Fig. S2c**). Salt stress hampered the LR emergence in Col-0 as more non-emerged
119 primordia were found under 125 mM NaCl (**Fig. 1c**). Compared to Col-0, *lbd16-1* displayed a
120 significantly lower proportion and density of emerged LR under both 75mM and 125 mM NaCl
121 (**Fig. 1c** and **Fig. S2c**), suggesting that LBD16 acts as a positive regulator of the LRP
122 emergence under salt stress.

123 We further analyzed the dynamic expression patterns of *LBD16* in the roots of four-
124 week-old *Arabidopsis* Col-0 wild-type plants after 0, 3, 6, 12, 18 and 24 h treatment with 125
125 mM NaCl. *LBD16* expression was enhanced after 3 h and peaked at 6 h after salt treatment
126 (**Fig.1d**). Further investigation of a promoter reporter line expressing *proLBD16::GUS* showed
127 that the promoter activity of *LBD16* was enhanced after 6 h salt treatment with 125 mM NaCl
128 in different regions of the primary root (**Fig. S3a**); from the elongation zone through the
129 differentiation zone, and up to the lateral root zone where lateral roots emerge (**Fig. S3b**).
130 Consistently, an $LBD16_{genomic}$*::GFP* (*lbd16-1*) fusion also revealed that *LBD16* expression was
131 enhanced in the main root elongation and differentiation zones by 125 mM NaCl (**Fig. 1e and**
132 **f**). Salt-induced *LBD16*-expressing cell types were not limited to the root stele but also found
133 in endodermis and cortex layers during LRP development in the differentiation zone and the
134 lateral root zone (**Fig. S3**), implying that LBD16 might play a role during LRP emergence to
135 pass through various root cell layers under salt. Taken together, salt may positively activate an

136 LBD16-mediated pathway in main root zones, which is required for plasticity of LR
137 development.

138 **Salinity activates an auxin-independent pathway mediating *LBD16* expression**

139 Since *LBD16* was previously shown to be involved in auxin-regulated LR
140 development[14], we first addressed the question whether salt would affect auxin signaling during
141 LR development. We used a high-resolution C3PO auxin reporter line that contains a three-
142 color reporter by incorporating a DR5v2::n3mTurqoise2 (auxin response) cassette into the
143 construct carrying the R2D2 (auxin input) cassette (pDR5v2:mTurquoise-
144 NLS/pRPS5a:mDII:ntdTomato/pRPS5a:DII:n3xVenus) to visualize auxin dynamics at cellular
145 level during LR development under salt stress[23]. We found that DR5v2 activity was reduced in
146 the root zones including meristem, elongation and early differentiation zones after 6 h treatment
147 with 125 mM NaCl (**Fig. 2a** and **b**), in accordance with decreased IAA levels in Col-0 roots
148 measured by liquid chromatography-tandem mass spectrometry (LC-MS/MS) after 6 h of 125
149 mM NaCl treatment (**Fig. 2c**). In the lateral root primordia, a significant reduction in the auxin
150 input R2D2 signal (indicated by mDII/DII) was also observed in Stage I and II after 6 h 125
151 mM NaCl treatment, while we did not detect significant changes in the auxin output signal
152 (DR5v2) in developing early stage LRP in response to salt (**Fig. S4a** and **b**). Although these
153 results are in line with salt inhibiting LR formation (**Fig. 1c** and **Fig. Sc**), they do raise the
154 question how salt enhances *LBD16* expression in roots (**Fig. 1e** and **f**) and whether this could
155 occur independent of auxin.

156 As *LBD16* expression in control conditions is induced by ARF7 and ARF19 acting
157 downstream of auxin, we evaluated *LBD16* expression in the *arf7-1;arf19-3* double knock-out
158 mutant. Interestingly, although under control conditions *LBD16* transcripts were decreased in
159 the *arf7-1;arf19-3* double mutant as compared with Col-0, after 6 h salt treatment *LBD16*
160 expression was increased in the *arf7-1;arf19-3* double mutant compared to Col-0 (**Fig.2d**). This
161 result implies that *LBD16* expression is regulated by an ARF7/ARF19 independent pathway
162 under salt conditions (**Fig.2d**). Since ARF7 was reported to be able to bind to the promoter
163 region of *LBD16* and regulate its expression[14], to further investigate the regulation of *LBD16*
164 by ARF7 under salt stress, we made use of a *ProARF7:ARF7-GR/arf7-1;arf19-1* transgenic
165 line with dexamethasone (DEX)-inducible ARF7 activity[14]. In control conditions, in line with
166 a previous study[14], *LBD16* expression was induced by the treatment with DEX plus IAA in the
167 roots of *ProARF7:ARF7-GR/arf7-1;arf19-1* seedlings, and this high expression was
168 maintained by the combination of IAA and DEX in the presence of the protein synthesis

169 inhibitor cycloheximide (CHX) to inhibit new protein synthesis of ARF7 (**Fig.2e**), suggesting
170 LBD16 is a primary target of ARF7 under control conditions. In response to salt stress, *LBD16*
171 expression was induced significantly by the combination of DEX and IAA in the presence of
172 CHX already early after 3 h treatment when compared with treatments with DEX and IAA
173 alone (**Fig.S4c**), indicating that LBD16 is primarily regulated by auxin-ARF7 signaling during
174 early salt response at 3 h. However, we observed that the presence of CHX together with DEX
175 and IAA to induce ARF7 activity was not able to promote *LBD16* expression after 6 h salt
176 treatment, and *LBD16* expression was significantly enhanced by salt in the roots of
177 *ProARF7:ARF7-GR/arf7-1;arf19-1* seedlings even without ARF7 activity under mock
178 treatment in the presence of CHX alone (**Fig. 2e**). These data support our hypothesis that
179 additional player(s) would regulate *LBD16* expression in response to a prolonged salt stress,
180 besides ARF7 and ARF19.

181 **Identification of novel upstream regulators of *LBD16* acting in response to salt stress**

182 To expand our understanding of the molecular mechanism underlying the salt-induced
183 LR plasticity phenotype of *lbd16* mutants and the observed salt-induced, auxin-independent
184 regulation of *LBD16* expression, we set out to identify possible additional upstream regulator(s)
185 of *LBD16* in response to salt stress. To this end, we performed yeast one hybrid (Y1H)
186 screening by using a 1309- bp promoter region upstream of the *LBD16* start codon as a bait,
187 and a collection of 1956 Arabidopsis transcription factors as prey to survey the putative
188 upstream regulators of *LBD16*[24]. As a result, more than 300 transcription factors were identified
189 to bind to the promoter region of *LBD16* with high presentation of bHLH, AP2-EREBP, C2H2
190 and MYB -type transcription factors (**Supplementary dataset 1** and Fig. **S5a**). To further
191 prioritize candidate transcription factors upstream of *LBD16* involved specifically in LR
192 development in response to salt stress, we carried out a comparative analysis of public
193 transcriptome datasets on root cell layers in response to salt stress[25] and gene expression during
194 LR development[26]. We found that 6499 out of 9193 salt-induced differentially expressed genes
195 (DEGs) in Arabidopsis root cell layers overlapped with genes induced during LR development
196 (9581 in total) (**Fig.3a**). We then compared these DEGs with putative LBD16 upstream
197 regulators including 91 candidates from our Y1H screening, and ARF7 and ARF19, which
198 resulted in a subset of 94 transcription factors including LBD16 itself that may be involved in
199 LR development in response to salt stress (**Fig.3a** and **Supplementary dataset 2**).

200 We next performed a network inference analysis to construct an *LBD16*-associated
201 network using GRNBoost2[27] based on the salt-induced time-series co-expression data of these

202 94 genes in the root stele cells from the salt response dataset[25](**Supplementary dataset 3**). To
203 test the robustness of the network prediction, we computed the network inference 100 times
204 and ranked all the predicted direct regulators of *LBD16* by how frequent they were predicted
205 as an *LBD16* upstream direct regulator. We also performed the same analysis using the
206 expression data under control conditions (**Supplementary dataset 3**). As a result, we were able
207 to identify 10 transcription factors that may regulate *LBD16* expression in control conditions,
208 and predicted 13 to act specifically in salt conditions (**Fig.3b**). Among the potential salt-specific
209 LBD16 upstream regulators, 5 of them were predicted with 100% frequency, including
210 AKS2(AT1G05805), ANAC001(AT1G01010), ZAT6(AT5G04340), BHLH007（AT1G03040）
211 and UNE12(AT4G02590) (**Fig. 3b** and **Supplementary dataset 3**).

212 To narrow down the salt-induced candidates for further functional characterization, we
213 performed an *LBD16* promoter analysis using the PlantPAN3.0 database to screen for upstream
214 transcription factors that were shown to bind the *LBD16* promoter directly in existing ChIPseq
215 experiments[28]. By comparative analysis of both the salt and control networks with the upstream
216 regulator candidates from PlantPAN3.0 (**Supplementary dataset 3**), we identified 4 candidate
217 salt-specific transcription factors that can directly bind the *LBD16* promoter; ZAT6
218 (AT5G04340), WOX13(AT4G35550), WRKY38 (AT5G22570), and DIV2 (AT5G04760) (**Fig.**
219 **3c**). Among these only ZAT6 was predicted with 100% frequency in our network analysis
220 (**Fig.3c and Supplementary dataset 3**). Further gene expression analysis showed that *ZAT6*
221 expression peaked at 3 h after 125 mM NaCl treatment prior to the salt-induced expression
222 peak of *LBD16* (**Fig. 1d and Fig.3d**), suggesting that *ZAT6* expression may be up-regulated as
223 early as 3 h after salt exposure to activate *LBD16* transcriptional activity at 6 h of salt treatment.
224 To examine whether ZAT6 is part of the *ARF7/19-LBD16* path, we also analyzed *ZAT6*
225 expression in the roots of the *arf7-1;arf19-3* double mutant and the *ProARF7:ARF7-GR/arf7-*
226 *1;arf19-1* line, and found that *ZAT6* expression was not affected by presence of ARF7 and
227 ARF19 in either control or salt conditions (**Fig. S5b** and **S5c**). Collectively, our results reveal
228 that ZAT6 is a potential novel upstream player regulating *LBD16* expression in response to
229 salinity in parallel with, but acting independently of ARF7 or ARF19.

230 **ZAT6 acts as a positive upstream regulator of *LBD16* in response to salt stress**

231 To understand the transcriptional regulation of *LBD16* by ZAT6, we further verified the
232 interaction of ZAT6 with the *LBD16* promoter using dual-luciferase assays in *Nicotiana*
233 *Benthamiana* leaves. We fused the 1309-bp region of the *LBD16* promoter to the FIREFLY
234 LUCIFERASE (LUC) to generate the reporter construct *pLBD16::LUC*. The *ZAT6* coding

235 region driven by the cauliflower mosaic virus (CaMV) 35S promoter was used as an effector
236 construct. Both the reporter and effector constructs together with the internal control RENILLA
237 LUCIFERASE (REN) driven by the 35S promoter were co-infiltrated into *N. benthamiana*
238 leaves using the *A. tumefaciens* AgL0 strain. Notably, co-infiltration of *35S::ZAT6* with
239 *pLBD16::LUC* resulted in a higher relative luciferase activity compared with an empty 35S
240 vector control (**Fig. 4a**). To understand whether ZAT6 is acting upstream of *LBD16* under salt
241 stress in *planta*, we assessed the expression of *LBD16* in roots of the loss-of-function mutants
242 *zat6-1* (SALK_061991C) and *zat6-2* (SALK_050196) as well as a constitutive repression line
243 of ZAT6 by using a SUPERMAN REPRESSIVE DOMAIN X (SRDX) fusion, namely
244 *35S::ZAT6::SRDX*. In both *zat6* mutant alleles (**Fig. S6a)**, a significant decrease in *LBD16*
245 expression was observed after 24 h of 125 mM NaCl treatment, while *LBD16* expression in
246 control conditions was not affected (**Fig.4b**). Similarly, *LBD16* expression in the
247 *35S::ZAT6::SRDX* line was significantly lower compared to Col-0 after 24h salt treatment
248 (**Fig.4c**). Together these results identify ZAT6 as a positive upstream regulator of *LBD16*,
249 which is required for the salt-induced increase in *LBD16* expression in roots.

250 To further investigate whether *ZAT6* is involved in LR formation under salinity, we
251 transferred 4-day-old seedlings of Col-0, *zat6-1* and *zat6-2* lines to agar plates containing 0
252 mM or 75 mM NaCl for 6 days and screened their RSA traits (**Fig. 4d** and **e**). No difference
253 was found in main root length or average lateral root length under either control or salt stress
254 conditions between Col-0 and the mutant plants (**Fig.4d and Fig. S6b, c**). Yet, a reduced
255 emerged LR density was observed in *zat6-1* and *zat6-2* mutants compared with Col-0 under 75
256 mM NaCl treatment (**Fig.4d, e**). The LR density reduction was evidently due to the reduction
257 in the number of emerged LRs under 75 mM NaCl (**Fig.S6d**), as the main root length did not
258 change significantly (**Fig. S6b**). We further evaluated LR development by scoring the emerged
259 LRs and non-emerged LRP in *35S::ZAT6::SRDX* line under both control and salt conditions.
260 We observed that the density of emerged LRs in the *35S::ZAT6::SRDX* line was significantly
261 decreased compared with Col-0 under 75 mM and 125 mM NaCl treatments whereas there was
262 no difference in main root length between these two genotypes **(Fig.4f** and **Fig.S7**), consistent
263 with the significantly lower *LBD16* expression in the *35S::ZAT6::SRDX* line compared with
264 Col-0 in response to salt stress (**Fig. 4c**). Similar to the *lbd16-1* mutant (**Fig.S2c)**, non-emerged
265 LR density was not reduced in the *35S::ZAT6::SRDX* line in response to salt stress while salt
266 suppressed the formation of LR in Col-0 (**Fig. 4f**). Collectively, the data suggest that *ZAT6* is
267 required for LRP development and LR emergence under salinity stress conditions.

268 **The *ZAT6-LBD16* pathway regulates cell wall remodeling during salt stress**

269 To gain insight into the molecular mechanisms of *LBD16*-mediated LR developmental
270 plasticity in response to salinity, we analyzed transcriptomes of roots of 8-day-old Col-0 and
271 *lbd16-1* mutant seedlings treated with 130 mM NaCl for 6 h by RNA sequencing (RNA-seq).
272 Further quality control analysis using principal component analysis (PCA) and hierarchical
273 clustering methods presented distinct expression patterns between salt and control conditions
274 (**Fig. S8a-c**). In total, 384 genes were differentially expressed (FDR≤0.05) between *lbd16-1*
275 and Col-0 in control conditions, while 1254 significant DEGs were observed under salt
276 treatment. Among these 1254 genes, 101 genes overlapped with DEGs in control condition and
277 1153 DEGs were found specifically for salt stress (**Fig.5a** and **Supplementary dataset 4**). To
278 identify key molecular processes involved in the salt-induced *LBD16*-mediated root branching
279 plasticity, we further performed gene ontology (GO) analyses for salt-specific DEGs
280 (**Supplementary dataset 4**). Strikingly, some of the most significantly overrepresented GO
281 terms we found were linked to cell wall organization (biological process, BP), cell wall (cellular
282 compartment, CC) and xyloglucosyl transferase activity (molecular function, MF) (**Fig. 5b,**
283 **Fig. S8d and Supplementary dataset 4**). Further investigation of the expression profiles of
284 the genes enriched in these cell-wall related GO terms suggested that salt stress more strongly
285 down-regulated the expression of pectin- and xyloglucan-related genes in the *lbd16-1* mutant
286 compared with Col-0, while a subtle difference in their expression profiles was observed
287 between *lbd16-1* and Col-0 in control conditions (**Fig. 5c)**. Among them, for example, *PME2*,
288 *GAUT7*, *XTH19* were previously shown to be expressed in developing LRs[7,29]. Consistently,
289 salt stress significantly enhanced the expression of *PME2* and *XTH19* in Col-0, whereas the
290 induction was abolished in the *35S::ZAT6::SRDX* line likely due to the repressed activity of
291 *LBD16* by ZAT6 (**Fig. 4c and Fig. S9**). Together, our data suggest that the ZAT6-*LBD16*
292 regulon is involved in salt-induced cell wall remodeling in response to salinity in roots.

293 To assess how the salt-induced *ZAT6-LBD16* pathway affects downstream cell wall
294 modification, we surveyed the cell wall monosaccharide composition changes in the roots of
295 Col-0, *lbd16-1*, *zat6-1* and *zat6-2* mutant lines in control conditions and after 24 h of 125 mM
296 NaCl treatment by high-performance anion-exchange chromatography with pulsed
297 amperometric detection (HPAEC-PAD) of isolated alcohol-insoluble residue cell wall material
298 (AIR). Salt exposure induced differences between Col-0 and *lbd16-1* in the relative amounts
299 of arabinose and galactose, while the relative xylose amount was increased in both lines after
300 salt treatment (**Fig. 5d**). Even if the overall salt-induced cell wall monosaccharide

301 composition in *zat6-1* and *zat6-2* relative to Col-0 was similar to that of the *lbd16-1* mutant,
302 we did not observe significant changes in the cell wall matrix composition of the *zat6* mutants
303 after 24 h or 72 h salt treatment (**Fig. S10**). Since we found salt-induced changes in *PME* and
304 *PMEI* gene expression in the *lbd16-1* mutant relative to Col-0 (**Fig. 5c**), which were reported
305 earlier to be highly relevant for LR development[7], we further assessed the degree of pectin
306 methylation in the roots of Col-0, *lbd16-1*, *zat6-1* and *zat6-2* mutant lines. We detected a
307 significantly higher degree of pectin methylation in Col-0 after 72 h salt treatment, while the
308 changes in *lbd16-1*, *zat6-1* and *zat6-2* mutant lines were much less noticeable (**Fig. 5e**). This is
309 in agreement with the fact that salt enhanced *PME2* expression in Col-0 whereas it is not altered
310 by salt in the *35S::ZAT6::SRDX* line, suggesting that PME2 expression is dependent on ZAT6
311 activity and that salt-induced regulation of pectin methylation requires LBD16 and ZAT6 (**Fig.
312 S9**). In summary, these data indicate that salt stress activates the *ZAT6-LBD16* module to
313 regulate downstream cell wall modification, positively contributing to LR developmental
314 plasticity under salinity.

315

316 **Discussion**

317 Plant lateral roots play important roles in acquisition of water and nutrients. Flexibility in
318 when and where to branch is essential for a plant to help reach optimal RSA for a dynamic soil
319 environment. We report here that *LBD16* plays a major role in mediating root branching
320 plasticity in response to salinity. We identified ZAT6 as a positive regulator that functions
321 independently of auxin-induced ARF7/19 signaling to induce *LBD16* expression in long-term
322 salt-stressed roots. Salt attenuates root auxin signaling since early stress response, whereas it
323 enhances the ZAT6-LBD16 module to facilitate downstream cell wall remodeling, likely to
324 promote LR development in response to salinity stress, bypassing the canonical root branching
325 pathways that function in control conditions (**Fig.5f**).

326 Auxin plays an essential role during LR formation and its downstream transcription factor
327 LBD16 was demonstrated to be required for LR initiation occurring in the early differentiation
328 zone of the *Arabidopsis* root[3,13]. Using the auxin reporter line C3PO, we provide evidence of
329 salt-suppressed auxin signaling (DR5v2 signals) in the main root zones where LRs are primed
330 (oscillation zone) and initiate (differentiation zone), and reduced auxin input signal (mDII/DII)
331 during the early stages of LRP development (Stage I through Stage IV) upon salt stress (**Fig.2a-
332 b, Fig.5a**). These data were further corroborated by the quantification of IAA content in salt-

333 stressed roots (**Fig. 2a**). The reduction in auxin signaling may contribute to the decreased
334 density of non-emerged LRP in Col-0 (**Fig. S2c**). However, salt did not affect the density of
335 non-emerged LRP in *lbd16-1* mutants (**Fig. S2c**), suggesting a positive role for LBD16 during
336 LR formation under salt conditions. In agreement with this, our data reveal that salt halts LRP
337 emergence leading to a decrease in emerged LR density in *lbd16-1* relative to Col-0 (**Fig. 1a-c**
338 **and Fig.S2c**). Moreover, salt-enhanced *LBD16* promoter activity and expression were not only
339 detected in the differentiation zone but also in the elongation zone (**Fig. 1e and Fig. 3a**),
340 suggesting LBD16 may have additional role(s) in the developmental processes prior to LR
341 initiation during salt stress, such as LR priming[3]. Due to reduced auxin signaling upon salt
342 stress, it is not likely auxin is the trigger for salt-induced *LBD16* expression (**Fig. 2a-c**).
343 Together, it appears that salt stress has an overall negative effect on auxin accumulation and
344 signaling in the main root zones involved in both LRP development and emergence, whereas
345 it also activates positively acting pathway(s) in which LBD16 is required to promote LRP
346 development under salinity. In the *lbd16* mutants, this positive contribution is lacking, resulting
347 in the observed reduced root branching phenotype.

348 Our network inference analysis indicates that, besides ARF7 and ARF19, various
349 transcription factors, such as ZAT6 (AT5G04340), WRKY38 (AT5G22570), WOX13
350 (AT4G35550) and DIV2 are potential LBD16 upstream regulators (**Fig. 3**). Among them, we
351 show that *ZAT6* might be involved in regulating LR density, by binding to the *LBD16* promoter
352 and upregulating *LBD16* expression in response to salt stress (**Fig. 4**). Although it is still
353 unknown how ZAT6 is activated by salt in plant roots, ZAT6 was previously found to be
354 expressed in the pericycle cells and to contribute to limiting Na^+ accumulation in the shoots
355 during salt stress[30]. ZAT6 was also reported to be phosphorylated directly by MITOGEN-
356 ACTIVATED PROTEIN KINASE 6 (MPK6) and implicated in regulation of seed germination
357 of Arabidopsis in saline conditions[31]. Salt may induce MPK6 activity within 15 min to activate
358 downstream salt-responsive gene expression in Arabidopsis seedlings[32]. In addition,
359 MPK3/MPK6 signaling is also involved in LR development via regulating downstream cell
360 wall remodeling pathways[17,33]. It is thus possible that salt might activate ZAT6 activity to
361 promote LR formation via the MPK6-mediated signaling pathway.

362 Our cell wall monosaccharide composition analyses did not detect significant cell wall
363 monosaccharide changes in the *zat6* mutant alleles in response to salt stress compared to Col-
364 0 (**Fig. S10**), which may be explained by the fact that ZAT6 acts upstream to activate *LBD16*
365 activity under salt to subsequently modulate the cell wall related genes. Nevertheless, salt

366 significantly upregulated the expression of cell wall remodeling genes such as *PME2* and
367 *XTH19* in Col-0, but not in the *35S::ZAT6::SRDX* line where both ZAT6 and LBD16 activities
368 are suppressed (**Fig. 4d and Fig. S9),** suggesting that the ZAT6 -LBD16 module plays a central
369 role in regulating cell wall remodeling genes under salt. Together with the similar pattern in
370 the degree of pectin methylation between *zat6* alleles and the *lbd16-1* mutants (**Fig.5e**), our
371 data support a role for *ZAT6* in cell wall remodeling, especially in affecting pectin methylation,
372 via LBD16. It is likely that the misregulation of cell wall-related genes by salt application and
373 consequent cell wall changes in the *zat6* and *lbd16-1* mutants compared to Col-0 may disturb
374 the cell wall loosening processes during LR emergence, resulting in the reduced LR density in
375 *zat6* and *lbd16* mutants compared to Col-0.

376 Although our results describe an auxin independent pathway controlling LR formation
377 during long-term salt stress, auxin-ARF7/19-LAX3 signaling was also previously shown to
378 induce expression of cell wall-related genes[16], and auxin signaling in the endodermal cell layer
379 is required to accommodate the swollen pericycle cells for LR initiation[34]. In addition, we
380 showed that during early salt stress, the auxin-ARF7/19 module may still mediate LBD16
381 expression (**Fig. 2e**). We also found auxin responsive genes such as *PIN3*(*AT1G70940*),
382 *LAX1*(*AT5G01240*) and several *IAAs* (*IAA9*, *IAA11* and *IAA13*) are present in the upregulated
383 GO term 'response to hormone' in our RNAseq analysis of *lbd16-1* mutants compared to Col-
384 0 specifically after 6 h salt treatment, but not in control conditions (**supplementary dataset 4**),
385 implying that there might be a feedback regulation of auxin signaling components during salt
386 response through unknown mechanism(s). Recently, SUMOylation of ARF7 during
387 hydropatterning was shown to block its binding activity to LBD16 and subsequently LR
388 formation[2]. In addition, salt stress might activate auxin downstream TOR signaling which is
389 required for LR formation by promoting the translation of ARF7/19 and LBD16[35,36]. Although
390 whether these above-mentioned post-transcriptional mechanisms could contribute to salt-
391 induced root branching phenotype of *lbd16* mutants is still unknown, our results do provide
392 evidence for a novel ZAT6-dependent transcriptional pathway to act independently of auxin in
393 controlling LR development in salt.

394 In summary, our data show that salt inhibits root auxin levels and signaling and in parallel
395 it activates alternative pathway(s) that help sustain root branching in salt. We have identified
396 such a pathway -a salt-activated *ZAT6-LBD16* bypath - promoting root branching in response
397 to salinity via altering cell wall remodeling. This provides a novel theoretical framework for
398 developmental plasticity under stress; we propose that the identified ZAT6-LBD16 module

399 allows plants to mitigate the effect of inhibition of the core developmental root branching
400 program by salt, allowing optimization of root architecture in stressful conditions.

401

402 # Methods

403 **Plant materials, growth conditions and stress treatments**

404 All the *Arabidopsis thaliana* wild-type, mutant and transgenic lines used in this research
405 are in Columbia-0 (Col-0) ecotype background, except for the auxin reporter line C3PO (in
406 Col-Utrecht ecotype)[23]. T-DNA knock-out insertion lines of *lbd16-1* (SALK_095791), *lbd16-*
407 *2* (SALK_040739) were obtained from the lab of Prof. Malcolm Bennett (University of
408 Nottingham) and Prof. Ben Scheres (Wageningen University& Research), respectively. Both
409 lines were genotyped again prior to being used in our study. T-DNA knock-out mutants of *zat6-*
410 *1* (SALK_061991C), *zat6-2* (SALK_050196) were obtained from the Nottingham Arabidopsis
411 Stock Centre (NASC, http://arabidopsis.info/) and genotyped for confirmation. The genomic
412 complementation line genomic *LBD16::GFP* line in *lbd16-1* (gLBD16) and
413 *pARF7::ARF7::GR* line was obtained from previously published report[13]. Primers used for
414 genotyping are listed in **Supplementary Table 1**.

415 For seedling pregrowth in petri dishes for all the root phenotyping experiments,
416 Arabidopsis seeds were surface sterilized in 70% (v/v) ethanol for 1 min, and then immersed
417 in 30% (v/v) bleach with triton X-100 (10 µL/50 mL) for 10 minutes and followed by washing
418 with sterilized MQ water for at least six times. Sterilized seeds were sown on 0.5x Murashige
419 and Skoog (MS) (including B5 vitamins, Duchefa Biochemie B.V.) media containing 1% (w/v)
420 2-(N-morpholino) ethanesulfonic acid (MES) (Duchefa Biochemie B.V.) with PH=5.8 and 0.8%
421 Plant Agar (Lab M, MC029), and then stratified at 4 ºC in dark for two days followed by pre-
422 growth at 21 ºC under 16 h light/8 h dark cycle and 65-70% humidity.

423 For LR phenotype characterization, 4-day-old seedlings were transferred to the medium
424 supplemented with 0 mM, 75 mM NaCl or 125 mM NaCl for 6 days.

425 For analyses of genomic *LBD16::GFP* expression patterns and *proLBD16::GUS*
426 expression, 6-day-old seedlings were transferred into liquid 0.5x MS medium containing 1%
427 (w/v) MES (Duchefa) (pH 5.8) with 0 mM or 125 mM NaCl on a shaker for 6 h to avoid
428 hypoxia during the treatments before further microscopic analysis.

429 For time course expression studies of *LBD16* and *ZAT6,* Col-0 plants were grown

430 hydroponically under 12 h/12 h light/dark cycle, 20°C until 4-week-old and then were treated
431 with 0 mM or 125 mM NaCl for 0 h, 3 h, 6 h, 12 h, 18 h or 24 h.

432 For the RNAseq analysis, seeds were sown and pre-grown on 11 cm x 11 cm nylon
433 mesh. Eight-day-old seedlings were transferred to 0.5x MS agar plates containing 1% (w/v)
434 MES (pH 5.8) and 1% Dashin Agar with 0 mM or 130 mM NaCl for 6 h before roots were
435 harvested for RNA isolation.

436 For cell wall analysis, seven-day-old seedlings of Col-0, *lbd16-1*, *zat6-1* and *zat6-2*
437 grown on 11 cm x 1 cm nylon mesh strips were transferred to 0.5x MS agar plates containing
438 1% (w/v) MES (pH 5.8) and 0.8% Plant Agar with 0 mM or 125 mM NaCl for 24 h or 3 days
439 (72 h) before roots were harvested for further analysis.

440 **Cloning and constructing**

441 For yeast-one-hybrid assay, a 1309-bp *LBD16* promoter sequence upstream of the start
442 codon was cloned into a gateway vector PDONR207 then was sequenced before the cassette
443 containing LBD16 promoter was recombined into a modified gateway compatible destination
444 bait vector pAbAi[37] containing the AbAr gene (AUR-1C) reporter through LR reaction, then
445 restriction enzyme digestions were performed to assess the final plasmid.

446 For *pLBD16::GUS* expression, *LBD16* promoter sequence was first cloned into
447 PDONR207 then combined into pFAST-G04 binary vector for plant transformation and
448 expression.

449 For *35S::ZAT6::SRDX* line, *ZAT6* coding sequence (with stop codon removed) was first
450 cloned into PDONR221, then subcloned into pGWB119 vector for plant transformation.

451 For luciferase assay, PDONR221 carrying the 1309-bp *LBD16* promoter sequence was
452 used for subcloning into pGWB435 carrying a LUC reporter; and PDONR221 carrying the
453 *ZAT6* coding sequence was used for subcloning into pH7WG2 binary vector for overexpression.

454 All constructs for plant transformation were transformed into *Agrobacterium*
455 *tumefaciens* AgL0 strain by electroporation and then transformed to Col-0 background by floral
456 dipping.

457 **Root system architecture assay**

458 Four-day-old seedlings of Col-0, *lbd16-1*, gLBD16 (in *lbd16-1*) complementation line,
459 *zat6-1* and *zat6-2* mutants were transferred to 0.5x MS media containing 0 mM, 75 mM or125
460 mM NaCl in square petri dishes, and were then placed in 70-degree racks and scanned on day

461 6 (10-day-old seedlings) after transferring. Main root and LR phenotypes were traced by
462 ImageJ with a Smartroot plugin[38]. Data were extracted in CSV files and then processed with R.

463 **Lateral root primordia assay**

464 Four-day-old seedlings of Col-0, *lbd16-1* and *35S::ZAT6::SRDX* lines were transferred
465 to 0.5x MS media containing 0 mM, 75 mM or 125 mM NaCl. Petri-dishes containing the
466 transferred seedlings were placed in 70-degree rack at 21ºC under 16 h light/8 h dark cycle and
467 65-70% humidity. For counting LRP and emerged LR under microscope, 6 days after
468 transferring, seedlings were fixed by immersion first in 20% (v/v) methanol with 4% (v/v)
469 hydrochloric acid at 57 °C for 20 min prior to immersion in 7% NaOH (w/v) in 60% (v/v)
470 ethanol at room temperature for 15 min, followed by rehydration in 40%, 20% and 10% (v/v)
471 ethanol for 5 min each. The fixed plants were stored in 10% ethanol at 4 ºC prior to microscopy
472 analysis. For microscopy analysis, Leica DM5200 microscope with Nomarski optics was used
473 and the roots were immersed in 50% (v/v) glycerol on microscopy slides for scoring LRP. The
474 LRP stages were determined according to previous report by Malamy and Benfey[5].

475 **Yeast one hybrid**

476 The final *pLBD16::AbAi* plasmid was transformed into pJ69-4α yeast strain as bait
477 DNA, and the yeast library containing CDS of 1956 Arabidopsis transcription factors cloned
478 into pDEST-22 vector was transformed into pJ69-4A yeast strain as prey proteins as previously
479 described[39]. Positive yeast colonies were selected and confirmed by using different synthetic
480 drop-out (SD) (Takara) media prepared according to the manufacturer's instructions. Prior to
481 screening, the strain carrying the *pLBD16::AbAi* bait was tested for autoactivation by using
482 empty prey strains carrying empty vector of pDEST-22 under various concentrations of
483 Aureobasidin A (AbA) (Takara) (0, 50 ng/mL,100 ng/mL, 150 ng/mL, 200 ng/mL and 400
484 ng/mL), and 200 ng/ml AbA was finally selected for further library screening. For mating-
485 based screening, all the the strains carrying the prey library were grown overnight in SD-Trp
486 medium in 96-well V bottom plates in a 28°C shaker. Yeast strain carrying the *pLBD16::AbAi*
487 bait DNA was grown in a 28°C shaker overnight in selective medium (SD-Ura). Mating of
488 yeast strains was carried out by spotting 5 μL 10-fold diluted overnight culture of both bait and
489 prey strains in one spot on agar plate containing SD-glu complete at 28°C for 2~3 days. The
490 diploid yeast strain colony spots contained both *pLBD16::AbAi* bait and prey proteins were
491 resuspend into 100 μL sterilized MQ and 5 μL was used to spot on selective agar media
492 containing SD-Trp-Ura and 200 ng/mL AbA at 28 °C. Positive interactions were observed after

493 2 to 3 days.

494 **Histochemical GUS Staining**

495 Six-days-old seedlings of *pLBD16::GUS* independent homozygous transformants in
496 Col-0 backgrounds were transferred to 0.5x MS liquid media containing 0 mM or125 mM NaCl
497 and placed on a shaker for 6 h during treatments. Then seedlings were transferred into GUS
498 staining buffer containing 50 mM sodium phosphate buffer (pH 7.2), 10 mM EDTA, 0.1% (v/v)
499 Triton X-100, 2.5 mM potassium ferri- and ferrocyanide, and 1 mg/mL 5-bromo4-chloro-3-
500 indolyl-b-glucuronic acid (Duchefa) and vacuumed for 15 min at room temperature before
501 incubation at 37°C for 1.5 h. Samples were cleared in clearing solution containing water (30
502 mL): chloral hydrate (80g):glycerol (10 mL) and mounted on microscope slides for imaging.
503 A Leica DM5200 microscope with Nomarski optics was used for imaging with 20x dry
504 objective.

505 **Confocal microscopy and auxin reporter analysis**

506 For the detection of genomic *LBD16::GFP* (in *lbd16-1* background), 6-day-old
507 seedlings were transferred to 0.5x MS liquid media containing 0 mM or 125 mM NaCl on a
508 shaker for 6 h to avoid hypoxia. After treatment, roots were fixed using 4% paraformaldehyde
509 (PFA) in 1 x PBS buffer for 1 h at room temperature with gentle agitation. After fixation, roots
510 were washed twice for 1 min in 1 x PBS buffer. Roots were then transferred and immersed in
511 ClearSee solution containing 10%(w/v) xylitol, 15% (w/v) sodium deoxycholate, and 25%
512 (w/v) urea at room temperature with gentle agitation overnight. Seedlings cell membranes were
513 counterstained for 30 min in a 0.1% Calcofluor white solution in ClearSee solution. Cleared
514 and stained roots were mounted on slides with ClearSee solution for confocal imaging.

515 For auxin response analysis during salt stress, seven-day-old Arabidopsis Col-0
516 seedlings carrying a triple color auxin reporter C3PO line[23] were transferred to 0.5x MS liquid
517 media containing 0 mM or 125 mM NaCl and placed on a shaker for 6 h. After treatment, roots
518 were fixed in PFA and cleared overnight using ClearSee solution. Cleared roots were mounted
519 on slides with ClearSee solution. Roots were visualized using a Leica TCS SP5II confocal laser
520 scanning microscope with a 40× NA = 1.20 water-immersion objective. mTurqoise2 and
521 Calcofluor white were excited using a 405 nm diode laser, mVenus and GFP were excited using
522 a 488nm Argon-ion laser, tdTomato was excited using a 552 nm laser. Detection was configured
523 as follows: Calcofluor white was detected at 410-430 nm; mTurqoise2 was detected at 468-495
524 nm; GFP was detected at 500-550 nm; Venus was detected at 524-540 nm; tdTomato was

525 detected at 571–630 nm. Z-stacks were acquired with 2.0 μm intervals, with the pinhole set to
526 2.0 Airy Unit. Virtual ratio images between channels were generated using the FIJI plugin
527 Calculator Plus (Fiji). Ratios between pixel signal intensities of nuclei were calculated on
528 SUM-slice projection of DII (C1;Venus) and mDII (C2;TdTomato) after subtracting
529 background signal (value=4). Nuclei in each LRP area were manually selected as 'Region of
530 interest' (ROI, Fiji) for quantifying average auxin input through ratio image (max C2/ max C1/
531 ROI) and average auxin output per ROI (max C3 / ROI).

532 **Luciferase assay**

533 Dual Luciferase Reporter (DLR) system (Promega) was employed to test the activation
534 of *pLBD16::LUC* by *35S::ZAT6*. Agrobacterium strains carrying *pLBD16::LUC*, *P19* gene-
535 silencing repressor and *35S::ZAT6* (using an empty vector containing 35S promoter as control)
536 constructs were co-infiltrated into leaves of four-week-old *Nicotiana Benthamiana*.
537 *35S::Renilla-luciferase* (REN) was used as an internal control for transformation efficiency.
538 Three days after infiltration, leaf samples of equal size were collected for protein extractions
539 using the Dual-Luciferase Reporter Assay System kit (Promega, Fitchburg, USA). Glomax 96
540 microplate luminometer (Promega, Fitchburg, USA) was used to measure the luciferase
541 activities. Using values from REN as internal control, the ratios were calculated.

542 **Public transcriptomic data analysis**

543 For the analysis of public microarray datasets of LR development[26] and root response
544 to salt stress[25], data analysis was performed using R with R packages provided by
545 Bioconductor[40]. The R packages affy and simpleaffy were employed for reading .CEL files of
546 the corresponding dataset, quality control, background adjustment and normalization[41,42].
547 Quality control was performed by checking whether the scale factors of different chips were
548 within 3-fold of one another and 3'/5' ratios of each sample were below 3 using simpelaffy[42].
549 GCRMA was used to perform global normalization[43]. Principal component analysis was
550 applied to check if the overall variability of the samples reflects their grouping. Based on the
551 affy_ATH1_array_elements-2010-12-20 table in TAIR, probe sets that were annotated to
552 hybridize to multiple loci in the Arabidopsis genome were removed from further analysis.
553 Differentially expressed genes were determined using the LIMMA package in R[44]. The
554 Benjamini-Hochberg method was used to correct for multiple testing. Genes with p-value ≤
555 0.001 and at least two-fold expression difference between contrasts were considered as
556 significantly differentially expressed genes (DEGs).

557 **Network inference**

558 Network inference was performed using GRNBoost2[27]. The overlapping genes from
559 public datasets and potential upstream regulators of *LBD16* from Y1H and published known
560 upstream regulator(s) were used as input for the network inference[14]. The expression data for
561 network inference were extracted from Geng et.al 2013[25] to predict the *LBD16* upstream
562 regulators under both control and salt conditions. Expression data from two timepoints for
563 control treatment and six timepoints for salt conditions were used for the network prediction.
564 To enhance the robustness of the network analysis, the algorithm was applied 100 times for
565 expression data under different conditions (control and salt conditions). For each run, predicted
566 direct regulators of *LBD16* were extracted from all inferred interactions using a custom Python
567 script. The frequency of each predicted *LBD16*-related interaction was calculated over these
568 100 times of prediction. To prioritize the list of potential regulators of *LBD16*, only interactions
569 with a frequency equal to or higher than 80% were listed for further analysis for the salt
570 conditions, and interactions with frequency ≥ 40% were selected under control conditions to
571 deal with higher variability in the network predictions (**Supplementary dataset 3**).

572 **RNAseq analysis**

573 8-day-old seedlings were treated with 0 mM or 130 mM NaCl for 6 h. Roots were
574 dissected for harvest and stored into liquid N_2 for RNA isolation. Approximately 40 roots were
575 pooled into one biological replicate. Total RNA was extracted using combined TRipure and
576 RNA isolation kit (Qiagen). Three biological replicates were used for sequencing.

577 Total RNA was used for RNA library preparation suitable for Illumina HiSeq paired
578 end sequencing using Illumina's TruSeq stranded mRNA kit for polyA mRNA selection. Then
579 mRNA was processed directly including RNA fragmentation, first and second strand cDNA
580 synthesis, adapter ligation and final library amplification according to the manufacturer's
581 protocol. The final library was eluted in 30 μL elution buffer followed by quality assessment
582 using a Bioanalyzer 2100 DNA1000 chip (Agilent Technologies) and quantified on a Qubit
583 quantitation platform (Life Technologies).

584 Prepared libraries were pooled and diluted to 6 pM for TruSeq Paired End v4 DNA
585 clustering on one single flow cell lane using a cBot device (Illumina). Final sequencing was
586 carried out on an Illumina HiSeq 2500 platform using 126, 7, 126 flow cycles for sequencing
587 paired end reads plus indexes reads. All steps for clustering and subsequent sequencing were
588 done according to the manufacturer's protocol. Reads were split per sample by using CASAVA

589 1.8 software (Illumina Inc, San Diego CA, USA). All sample preparations and sequencing were
590 done by the Genomics lab of Wageningen University and Research, Business Unit Bioscience.

591 Read quality was assessed using FastQC
592 (https://www.bioinformatics.babraham.ac.uk/projects/fastqc/) and low-quality reads were
593 removed using "trim galore!"
594 (https://www.bioinformatics.babraham.ac.uk/projects/trim_galore/). Reads were mapped to
595 the Arabidopsis TAIR10 transcriptome using Salmon[45].

596 Differential gene expression was quantified using DESeq2[46] under different contrasts
597 (*lbd16-1* vs Col0 in both control and salt conditions) using a false discovery rate (FDR) cut-off
598 of 0.05. The counts of the top 5000 differentially expressed genes (DEGs) were used for
599 principal component analysis. Expression heatmap of sample-to-sample distances was
600 calculated from the Log_2 transformed count data for overall gene expression. Clustering of 12
601 RNA-seq samples was carried out to show the overview of relationships between genotypes.
602 GO enrichment analysis was performed for the NaCl-induced DEGs in *lbd16-1* vs Col-0 by
603 using the R package gProfiler[47].

604 **Gene expression study**

605 For expression studies of *LBD16* in Col-0, *pARF7::ARF7::GR* in *arf7-1;arf19-1* double
606 mutant line, *zat6-1*, *zat6-2,* and *35S::ZAT6::SRDX* line, 7-day-old seedlings pregrown on mesh
607 strips were transferred to 0.5x MS agar plates containing 0 mM or 125 mM NaCl. The root
608 samples were collected after 3 h, 6 h or 24 h treatment as specified in the figure legends for
609 further analysis. For *LBD16* expression in *arf7-1;arf19-3* line, 5-day-old seedlings grown on
610 mesh were transferred to 0 mM or 130 mM NaCl before roots were harvested for RNA
611 extraction.

612 For time course gene expression study of *LBD16* and *ZAT6*, roots of 4-week-old
613 hydroponically grown Col-0 plants were harvested after treated with 0 mM or 125 mM NaCl
614 for 0 h, 3 h, 6 h, 12 h, 18 h and 24 h for RNA isolation.

615 For expression studies on *pARF7::ARF7::GR* in *arf7-1;arf19-1* double mutant lines, 7-
616 day-old seedlings pregrown on mesh strips were transferred to 0.5x MS agar plates containing
617 0 mM or 125 mM NaCl for 3 h or 6 h before roots were harvested for RNA isolation.

618 Total RNAs were extracted with RNA isolation kits (NZYtech, Portugal). The RNA
619 quality and concentration were assessed prior to cDNA synthesis. iScript cDNA synthesis kit
620 (Bio-Rad) was used for cDNA synthesis. The primers used in qRT-PCR are listed in

621 **Supplementary table 1.** 2x qPCRBIO SyGreen Mix Lo-ROX (PCRBIOSYSTEMS, UK) was
622 used for qRT-PCR analysis. qRT-PCR analyses were performed using the CFX96 or CFX384
623 connect real-time PCR detection system (Bio-Rad).

624 **IAA measurement**

625 Seven-day old seedlings were transferred to fresh 0.5x MS agar plates supplemented
626 with 0 mM or 125 mM NaCl (Duchefa). After 1, 3, 6, 12 h being transferred, roots were
627 dissected with a sharp blade, weighed, flash frozen in liquid N_2 and stored at -80 °C for further
628 analysis. For IAA extraction, approximately 60 roots (11.8±3.0 mg) were pooled in one
629 biological replicate. Frozen material was ground to a fine powder and further extracted with 1
630 mL of 10% methanol containing 100 nM ^{13}C-labeled IAA internal standard. The extraction was
631 carried out according to a previous report with minor modification[48]. Namely, a StrataX 30
632 mg/3 mL spe-column (Phenomenex) was used.

633 For detection and quantification of IAA by liquid chromatography-tandem mass
634 spectroscopy, sample residues were dissolved in 100 µL acetonitrile /water (20:80 v/v) and
635 filtered using a 0.2 µm nylon centrifuge spin filter (BGB Analytik). IAA was identified and
636 quantified by comparing retention time and mass transitions with IAA standard using a Waters
637 XevoTQS mass spectrometer equipped with an electrospray ionization source coupled to an
638 Acquity UPLC system (Waters) as previously described[49]. Chromatographic separations were
639 conducted using acetonitrile/water (containing 0.1% formic acid) on a Acquity UPLC BEH
640 C18 column (2.1 mm x100mm, 1.7 µm, Waters) at 40°C with a flowrate of 0.25 mL/min. The
641 column was equilibrated for 30 min with acetonitrile /water (20:80 v/v) containing 0.1% formic
642 acid. Samples were analyzed by injecting 5 µL, followed by the elution using program of 17
643 min in which the acetonitrile fraction linearly increased from 20% (v/v) to 70% (v/v). The
644 column was washed after every sample by increasing the acetonitrile fraction to 100% in one
645 minute and maintaining this concentration for 1 min. The acetonitrile fraction was reduced to
646 20% in one minute and maintained at this concentration for one minute before injecting the
647 next sample. The capillary voltage was set at 3.5 kV, the source temperature and the desolvation
648 temperature at 150 °C and 350 °C, respectively. Multiple reaction monitoring (MRM) was used
649 for identification and quantification by comparing retention times and MRM transitions
650 (+176.25>103.2; +176.25>130.2) with IAA standard. MRM transitions and cone voltages (30v)
651 were set using the IntelliStart MS Console. Data acquisition and analysis were carried out using
652 MassLynx 4.1 (TargetLynx) software (Waters) and was further processed in excel. The final
653 IAA content in each sample was normalized by the corresponding internal standard recovery

654 and sample weight. All values were normalized to the 1 h control timepoint.

655 **Cell wall analysis**

656 Seven-day-old seedlings of Col-0, *zat6-1*, *zat6-2* and *lbd16-1* were transferred to 0.5x
657 MS agar plates containing 0 mM or 125 mM NaCl. Roots were harvested into 2 mL tubes after
658 24 h or 72 h treatment with 0 mM or 125 mM NaCl and ground homogenously. 1 mL of pre-
659 warmed 70% (v/v) ethanol was added to the tubes followed by vortexing. This solution was
660 spun at max speed for 30 seconds and the supernatant discarded, after which this ethanol
661 washing step was repeated and the supernatant was discarded again. A mixture of 50% (v/v)
662 chloroform and 50% (v/v) methanol was added to the pellet, and the tube mixed by gently by
663 inverting the tube at least 5 times. Tubes were spun at max speed for 30 seconds, and the
664 supernatant was discarded. Acetone was added to the tubes, the tubes spun at max speed for 30
665 seconds, and the supernatant was discarded. This acetone wash was repeated 3 times. Tubes
666 are left to dry with open lids overnight in a fume hood. The resulting alcohol insoluble residues
667 (AIR) were used for further analysis.

668 For analysis of cell wall monosaccharide composition, 1-2 mg AIR was weighed out in
669 2 mL screw caps tubes and used for extraction of neutral cell wall sugars and uronic acids as
670 described[50]. High-performance anion-exchange chromatography with pulsed amperometric
671 detection (HPAEC-PAD) was performed on a biocompatible Knauer Azura HPLC system,
672 equipped with an Antec Decade Elite SenCell detector. Monosaccharides were separated on a
673 Thermo Fisher Dionex CarboPac PA20 column BioLC guard (3 x 30 mm) and analytical (3 x
674 150 mm) column as previously described (https://doi.org/10.1073/pnas.2119258119). Briefly,
675 samples were diluted with ultrapure water, ribose was added as an internal standard and
676 separation performed with a solvent gradient of (A) water, (B) 10 mM NaOH and (C) 700 mM
677 NaOH at 0.4 mL /min flow rate. 0 to 25 min: 20% B, 25 to 28 min: 20 to 0% B, 0 to 70% C,
678 28 to 33 min: 70 % C, 33 to 35 min: 70 to 100% C, 35 to 38 min: 100% C, 38 to 42 min: 0 to
679 20% B, 100 to 0% C, 42 to 60 min: 20% B.

680 The degree of pectin methyl-esterification was analyzed as described[51] with minor
681 modifications. 1 mg AIR was saponified in 0.2 mL 250 mM NaOH for 1h at room temperature
682 and neutralized with HCl. After centrifugation, 50 µL diluted supernatant was incubated with
683 an equal volume of 0.1 M sodium phosphate buffer (pH 7.5) containing 0.03 units alcohol
684 oxidase (Sigma A2404) for 15 min at room temperature under shaking. After addition of 100
685 µL 0.02 M 2,4-pentanedione in 2 M ammonium acetate and 0.5 M acetic acid, samples were

686 incubated at 68°C for 10 min, briefly cooled on ice and transferred in 96-well microtiter plates.
687 Absorbance was measured at 412 nm in a Tecan infinite 200Pro microplate reader and
688 calibrated against a 0-350 µM formaldehyde standard series. The degree of pectin methyl-
689 esterification was calculated as the molar ratio of methanol to uronic acid determined via
690 HPAEC-PAD analysis.

691 **Statistical analysis**

692 Graph Pad Prism software and R were used for statistical analysis. For the proportion
693 of non-emerged LRP and emerged LRs a generalized linear model was fitted (glm(cbind(`non-
694 emerged`,emerged) ~ genotype*condition , family = binomial(link = "logit")) and statistical
695 differences were derived from least squares mean analysis with custom contrast (emmeans R
696 package 1.8.1-1).

697

698 Author contributions

699 Y.Z. and C.T. conceived the project. Y.Z. performed most of the experiments and the
700 data analysis. Y.L. performed the network inference under the supervision of A.D.J.D and Y.Z.
701 Y.L conducted RNAseq data analysis, assisted by J.L.. T.Z. assisted with the experiments and
702 performed confocal microscope analyses. K.D. contributed to the qRT-PCR analysis and
703 phenotypic analysis of the *35S::ZAT6::SRDX* lines. D.K. performed the phenotypic analysis of
704 the *lbd16-2* allele and assisted the statistical analysis for Fig.1c. J.L. and F.V. performed IAA
705 analysis. K.M. and T.E. contributed the cell wall monosaccharide composition analysis. H.L.,
706 J.M., N.G-B, J.Y., Yu.Z. Y.W., T.G., and J.W assisted with experiments and data analysis.
707 A.D.J.D supervised the network inference and contributed to the RNAseq data analysis. Y. Z
708 and C.T. acquired the funding, guided the research and wrote the manuscript. All authors
709 approved the manuscript.

710

711 Acknowledgements

712 We would like to thank Malcolm Bennett (University of Nottingham) for kindly
713 providing us the *gLBD16::GFP* (*lbd16-1*) line and *arf7-1;arf19-3* double mutant, Tom
714 Beeckman (Ghent University) and Hidehiro Fukaki for sharing with us the *pARF7::ARF7::GR*
715 (*arf7-1;arf19-1*) line, and Dolf Weijers (Laboratory of Biochemistry, Wageningen University
716 & Research) for providing the C3PO line. We thank Elio Schijlen (Bioscience, Wageningen

University & Research) for the assistance in library preparation and RNA sequencing. This work is supported by the European Research Council (ERC) (grant agreement 724321), Dutch Research Council (NWO) Vici grant (Grant VI.C.192.033) and NWO-ENW KLEIN (OCENW.KLEIN.421), Netherlands Organisation for Health Research and Development (ZonMW) Enabling Technologies Hotels programme- early career scientists projects (Grant No.435004012) and a China Scholarship Council (CSC) - Sino-Dutch Bilateral Exchange Scholarship (CF 13731).

Competing interests

No competing interests to declare.

728 ## Figure legends

729 **Fig. 1 Identification of LBD16 as a mediator for LR development in response to salinity**.
730 **a-c**, Phenotypical analysis of emerged LRs (ELR) and non-emerged LRP (NE) in Col-0 and
731 *lbd16-1* in control and salt conditions. **a**, Representative images of root phenotypes of *lbd16-1*
732 compared with Col-0 and *lbd16-1* mutant in control and salt conditions (0 mM, 75 mM NaCl
733 and 125 mM NaCl). Scale bars represent 1cm. **b,** Density of ELR in Col-0 and *lbd16-1* mutant
734 in control and salt conditions (0 mM,75 mM and 125 mM NaCl) (n= 20~25). **c,** Distribution of
735 ELR and NE LRP in Col-0 and *lbd16-1* mutant in control and salt conditions (0 mM, 75 mM
736 and 125 mM NaCl). Data represents a pool of 4 independent experiments (in each experiment
737 n=7~13). **d**, Salt-induced *LBD16* expression patterns in 4-week-old hydroponically grown Col-
738 0 wild-type plants (n=4~5). Relative expression was normalized by both house-keeping gene
739 *At2g43770* and expression at 0 h timepoint. **e,** Expression pattern of genomic *LBD16::GFP*
740 fusion in root zones after treated with 0 mM and 125 mM NaCl for 6h. **f,** Quantification of
741 *gLBD16::GFP* intensities in root zones. Data in **b-d** and **f** represent means ± SEM. Statistical
742 analysis in **b** was done using two-way ANOVA followed by Tukey's multiple comparison tests.
743 Statistical analysis in **c** was done by fitting a generalized linear model. Statistical analyses in **d**
744 and **f** were done using two-sided Student's T-test. * $P < 0.05$, ** $0.05<P<0.01$, *** $P<0.01$,
745 **** $P<0.001$. Data in a-f represents multiple independent experiments. Scale bars represent
746 100μm in **e**.

747 **Fig. 2 Salinity activates an auxin-independent pathway mediating *LBD16* expression. a,**
748 auxin output signals indicated by DR5v2 in main root zones. **b,** Quantification of DR5v2 signal
749 intensity in root zones including meristem, elongation zone, and (early) differentiation zone. **c,**
750 Relative IAA content normalized by internal standard in the roots of 7-day-old Col-0 seedlings
751 by LC-MS/MS after 1, 3, 6 and 12 h 125 mM NaCl treatment (n=4). **d,** Relative expression of
752 *LBD16* compared with Col-0 under control condition in the roots of 5-day-old seedling of *arf7-*
753 *1;arf19-3* double mutants and Col-0 plants after 6 h 130 mM NaCl treatment (n=4~5). **e,**
754 Relative expression of *LBD16* in the *pARF7::ARF7::GR* (in *arf7-1;arf19-1*) plants were treated
755 with 1 μM *IAA*, 2 μM dexamethasone (DEX) and/or 10 μM cycloheximide (CHX) inducible
756 lines in control and salt conditions after 6h 125 mM NaCl treatment in comparison with Mock
757 treatment . Expression values were normalized by house-keeping gene *At2g43770* in c and d.
758 Statistical analyses in **b** and **c** were done using two-sided Student's T-test. Statistical analyses
759 in **d and e** were done using two-way ANOVA, respectively. * $P < 0.05$, ** $0.05<P<0.01$.

760 **Fig. 3 Identification of novel upstream regulators of LBD16 in response to salt stress. a,**
761 novel upstream regulators of *LBD16* mediating LR development in response to salt stress were
762 selected by a comparative analysis among salt-induced root cell-types specific transcriptomic
763 response[25], LR development-associated genes[26] and putative *LBD16* upstream regulators via
764 yeast one-hybrid screening among 1956 *Arabidopsis* transcription factors[24]. **b**, Network
765 inference prediction of LBD16 upstream direct regulators by GRNBoost2 under control and
766 salt conditions. The topology of the network shows genes that could directly regulate *LBD16*.
767 Color (blue) intensity indicates the robustness of the network prediction (100% to 40%). **c**,
768 Comparative analysis of the *LBD16*-associated upstream network with *LBD16* promoter
769 analysis on the basis of ChIP-seq evidences in PLANTPAN3.0[28]. **d,** Salt-induced expression
770 pattern of one of the novel upstream regulators *ZAT6*. Data were collected using roots of 4-
771 week-old hydroponically grown Col-0 plants normalized by house-keeping gene *At2g43770*
772 and expression of 0 h time point (n=4). Statistical analysis in **d** was done using two-sided
773 Student's T-test. * $P < 0.05$, ** $0.05<P<0.01$.

774 **Fig. 4 ZAT6 acts upstream of LBD16 in response to salt stress. a,** Overexpression of *ZAT6*
775 (*35S::ZAT6*) enhanced LUC expression driven by *LBD16* promoter in *Nicotiana Benthamian*
776 leaves (n=5). **b,** Relative expression of *LBD16* in response to 125 mM NaCl treatment in Col-
777 0, *zat6-1* and *zat6-2* mutant alleles quantified by RT-qPCR. **c**, Expression of *LBD16* in roots of
778 *35S::ZAT6::SRDX* line after 24 h treatment by mock and salt (125 mM NaCl) conditions
779 (n=4~5 pools of 60 roots). **d**, Representative images of root phenotypes of Col-0, *zat6-1* and
780 *zat6-2* mutants under mock and 75 mM NaCl. Scale bars represent 1cm. **e,** Emerged LR density
781 of *zat6-1* and *zat6-2* mutants compared with Col-0 under mock and 75 mM NaCl. Data were
782 collected from 3 independent experiments (3 pools of 20~25 roots). **f,** Density of emerged LRs
783 and non-emerged LRP in Col-0 and *35S::ZAT6::SRDX* line under mock, 75 mM NaCl and 125
784 mM NaCl conditions (n=10~11). Data represent results of two independent experiments
785 (n=10~13). Data in **a**, **b**, **c**, **e** and f represent means ± SEM. Expression data in **b** and **c** were
786 obtained from 4 biological replicates (approx. 40~45 roots were pooled as one replicate) and
787 presented as the relative expression to mock condition after normalization by the reference
788 gene *At2g43770*. Root RNA samples were obtained from 7-day old seedlings transferred to
789 0.5x MS medium supplemented with 0 or 125 mM NaCl for 24 h. Statistical analyses in a and
790 b were done using two-sided Student's T-test. Statistical analyses in **c, e** and **f** were done using
791 two-way ANOVA, followed by Tukey's multiple comparison tests. * $P < 0.05$, ** $0.05<P<0.01$,
792 *** $P<0.01$, **** $P<0.001$.

Fig. 5 The *ZAT6-LBD16* path regulates cell wall remodeling during salt stress. a, Venn diagram representing the number of differentially expressed genes (DEGs) comparing 8-day-old *lbd16-1* mutant with Col-0 after treatment with 0 mM and 130 mM NaCl for 6 h (no cutoff for log-fold changes, P <0.05). **b,** GO term analysis of the 1153 salt-induced genes in **a**. BP, biological process; CC, cellular compartment; MF, molecular function. Y-axis indicates the significance of the GO terms. X-axis indicates term size. **c**, Heatmaps showing the relative expression of genes listed in pectin- and xyloglucan-related GO terms in the roots of Col-0 and *lbd16-1* in control and salt conditions. **d,** Cell wall monosaccharides analysis of roots of 7-day old *lbd16-1* and Col-0 after transferring to agar plates containing 0 mM or 125 mM NaCl for 24 h. Data are mean ± SEM. Data were obtained from 4 independent biological replicates containing 60 ~80 roots. Statistical analysis was done using two-way ANOVA, followed by Tukey's multiple comparison tests. * P < 0.05, ** 0.05<P<0.01, *** P<0.01. **e,** The degree of pectin methylation in Col-0, *lbd16-1*, *zat6-1* and *zat6-2* lines under mock and 125 mM NaCl conditions. Data were collected from roots of 7-day old seedlings after transferring to 0 mM or 125 mM NaCl for 72 h (n=4 pools of 60 ~80 roots). **f,** Schematic diagram of LBD16-mediated molecular network in the main zones guiding lateral root development under control (indicated by black arrows) and salt stress conditions (indicated by blue arrows). The blue dashed boxes highlight the molecular pathways identified by this study. Under control condition, auxin and its downstream response factor ARF7 was reported to be involved in cell wall remodeling process during lateral root development[16], in which the role of LBD16 was unclear. During early salt stress (< 3h) response, root auxin signaling is inhibited while auxin signaling is still contributing to the regulation of LBD16. Meanwhile, salt activates ZAT6 which is further regulating LBD16 during long-term (> 3h) salt stress response to mediate downstream cell wall remodeling and subsequently lateral root development. Various root cell layers were presented by different colors. White, yellow, purple, light green and dark green represent stele (Ste), pericycle (Pe), endodermis (En), cortex (Co) and epidermis (Epi), respectively. MZ, EZ, DZ and LRZ denote meristematic zone, elongation zone, differentiation zone and lateral root zone (root zone with emerged LRs), respectively.

References

1. Julkowska, M.M. *et al.* Genetic Components of Root Architecture Remodeling in Response to Salt Stress. *Plant Cell* **29**, 3198-3213 (2017).

2. Orosa-Puente, B. *et al.* Root branching toward water involves posttranslational modification of transcription factor ARF7. *Science* **362**, 1407-1410 (2018).

827 3. Du, Y. & Scheres, B. Lateral root formation and the multiple roles of auxin. *J Exp Bot* **69**, 155-167 (2018).

828 829 4. Banda, J. *et al.* Lateral Root Formation in Arabidopsis: A Well-Ordered LRexit. *Trends Plant Sci* **24**, 826-839 (2019).

830 831 5. Malamy, J.E. & Benfey, P.N. Organization and cell differentiation in lateral roots of Arabidopsis thaliana. *Development* **124**, 33-44 (1997).

832 833 6. J. K. Bell, M.E.M. A histological study of lateral root initiation and development inZea mays. *Protoplasma* **70**, 26 (1970).

834 835 7. Wachsman, G., Zhang, J., Moreno-Risueno, M.A., Anderson, C.T. & Benfey, P.N. Cell wall remodeling and vesicle trafficking mediate the root clock in Arabidopsis. *Science* **370**, 819-823 (2020).

836 837 8. Ramakrishna, P. *et al.* EXPANSIN A1-mediated radial swelling of pericycle cells positions anticlinal cell divisions during lateral root initiation. *Proc Natl Acad Sci U S A* **116**, 8597-8602 (2019).

838 839 9. Lee, H.W. & Kim, J. EXPANSINA17 up-regulated by LBD18/ASL20 promotes lateral root formation during the auxin response. *Plant Cell Physiol* **54**, 1600-11 (2013).

840 841 842 10. Lee, H.W., Kim, M.J., Kim, N.Y., Lee, S.H. & Kim, J. LBD18 acts as a transcriptional activator that directly binds to the EXPANSIN14 promoter in promoting lateral root emergence of Arabidopsis. *Plant Journal* **73**, 212-224 (2013).

843 844 11. Lavenus, J. *et al.* Lateral root development in Arabidopsis: fifty shades of auxin. *Trends Plant Sci* **18**, 450-8 (2013).

845 846 12. Santos Teixeira, J.A. & Ten Tusscher, K.H. The Systems Biology of Lateral Root Formation: Connecting the Dots. *Mol Plant* **12**, 784-803 (2019).

847 848 849 13. Goh, T., Joi, S., Mimura, T. & Fukaki, H. The establishment of asymmetry in Arabidopsis lateral root founder cells is regulated by LBD16/ASL18 and related LBD/ASL proteins. *Development* **139**, 883-893 (2012).

850 851 14. Okushima, Y., Fukaki, H., Onoda, M., Theologis, A. & Tasaka, M. ARF7 and ARF19 regulate lateral root formation via direct activation of LBD/ASL genes in Arabidopsis. *Plant Cell* **19**, 118-30 (2007).

852 853 15. Porco, S. *et al.* Lateral root emergence in Arabidopsis is dependent on transcription factor LBD29 regulation of auxin influx carrier LAX3. *Development* **143**, 3340-3349 (2016).

854 855 16. Kumpf, R.P. *et al.* Floral organ abscission peptide IDA and its HAE/HSL2 receptors control cell separation during lateral root emergence. *Proc Natl Acad Sci U S A* **110**, 5235-40 (2013).

856 857 17. Zhu, Q. *et al.* A MAPK cascade downstream of IDA-HAE/HSL2 ligand-receptor pair in lateral root emergence. *Nat Plants* **5**, 414-423 (2019).

858 859 18. Xu, P. & Cai, W. Nitrate-responsive OBP4-XTH9 regulatory module controls lateral root development in Arabidopsis thaliana. *PLoS Genet* **15**, e1008465 (2019).

860 861 19. Kawa, D. *et al.* Phosphate-Dependent Root System Architecture Responses to Salt Stress. *Plant Physiol* **172**, 690-706 (2016).

862 863 20. Julkowska, M.M. *et al.* Capturing Arabidopsis root architecture dynamics with ROOT-FIT reveals diversity in responses to salinity. *Plant Physiol* **166**, 1387-402 (2014).

864 865 21. Zolla, G., Heimer, Y.M. & Barak, S. Mild salinity stimulates a stress-induced morphogenic response in Arabidopsis thaliana roots. *J Exp Bot* **61**, 211-24 (2010).

866 867 868 22. Lee, H.W., Kim, N.Y., Lee, D.J. & Kim, J. LBD18/ASL20 regulates lateral root formation in combination with LBD16/ASL18 downstream of ARF7 and ARF19 in Arabidopsis. *Plant Physiol* **151**, 1377-89 (2009).

869 870 871 872 23. Jesse J. Küpers, B.L.S., Lisa Oskam, Chrysoula K. Pantazopoulou, Sanne E. A. Matton, Emilie Reinen, Che-Yang Liao, Eline D.C. Eggermont, Harold Weekamp, Wouter Kohlen, Dolf Weijers, Ronald Pierik. Local light signalling at the leaf tip drives remote differential petiole growth through auxin-gibberellin dynamics. *bioRxiv* (2022).

873 874 24. Pruneda-Paz, J.L. *et al.* A genome-scale resource for the functional characterization of Arabidopsis transcription factors. *Cell Rep* **8**, 622-32 (2014).

875 25. Geng, Y. *et al.* A spatio-temporal understanding of growth regulation during the salt stress response in

Arabidopsis. *Plant Cell* **25**, 2132-54 (2013).

26. Voss, U. *et al.* The circadian clock rephases during lateral root organ initiation in Arabidopsis thaliana. *Nat Commun* **6**, 7641 (2015).

27. Moerman, T. *et al.* GRNBoost2 and Arboreto: efficient and scalable inference of gene regulatory networks. *Bioinformatics* **35**, 2159-2161 (2019).

28. Chow, C.N. *et al.* PlantPAN3.0: a new and updated resource for reconstructing transcriptional regulatory networks from ChIP-seq experiments in plants. *Nucleic Acids Res* **47**, D1155-D1163 (2019).

29. Atmodjo, M.A. *et al.* Galacturonosyltransferase (GAUT)1 and GAUT7 are the core of a plant cell wall pectin biosynthetic homogalacturonan:galacturonosyltransferase complex. *Proc Natl Acad Sci U S A* **108**, 20225-30 (2011).

30. Maria Amparo Asensi Fabado, E.A.A., Liam Walker, Giorgio Perrella, Graham Hamilton, Pawel Herzyk, Miriam L Gifford, Anna Amtmann. Cell-type specific transcriptional networks in root xylem adjacent cell layers. *bioRxiv* **2022.02.04.479129**(2022).

31. Liu, X.M. *et al.* Phosphorylation of the zinc finger transcriptional regulator ZAT6 by MPK6 regulates Arabidopsis seed germination under salt and osmotic stress. *Biochem Biophys Res Commun* **430**, 1054-9 (2013).

32. Gigli-Bisceglia, N., van Zelm, E., Huo, W., Lamers, J. & Testerink, C. Arabidopsis root responses to salinity depend on pectin modification and cell wall sensing. *Development* (2022).

33. Huang, R. *et al.* Noncanonical auxin signaling regulates cell division pattern during lateral root development. *Proc Natl Acad Sci U S A* **116**, 21285-21290 (2019).

34. Vermeer, J.E.M. *et al.* A Spatial Accommodation by Neighboring Cells Is Required for Organ Initiation in Arabidopsis. *Science* **343**, 178-183 (2014).

35. Michael Stitz, D.K., Maximilian Reinert, Mikhail Schepetilnikov, Béatrice Berthet, Jazmin Reyes-Hernández, Denis Janocha, Anthony Artins, Marc Boix, Rossana Henriques, Anne Pfeiffer, Jan Lohmann, Emmanuel Gaquerel, Alexis Maizel. TOR acts as a metabolic gatekeeper for auxin-dependent lateral root initiation in Arabidopsis thaliana. *EMBO J.* **e111273**(2023).

36. Jamsheer, K.M. *et al.* A negative feedback loop of TOR signaling balances growth and stress-response trade-offs in plants. *Cell Rep* **39**, 110631 (2022).

37. Danisman, S. *et al.* Arabidopsis class I and class II TCP transcription factors regulate jasmonic acid metabolism and leaf development antagonistically. *Plant Physiol* **159**, 1511-23 (2012).

38. Lobet, G., Pages, L. & Draye, X. A Novel Image-Analysis Toolbox Enabling Quantitative Analysis of Root System Architecture. *Plant Physiology* **157**, 29-39 (2011).

39. de Folter, S. & Immink, R.G. Yeast protein-protein interaction assays and screens. *Methods Mol Biol* **754**, 145-65 (2011).

40. Gentleman, R.C. *et al.* Bioconductor: open software development for computational biology and bioinformatics. *Genome Biol* **5**, R80 (2004).

41. Gautier, L., Cope, L., Bolstad, B.M. & Irizarry, R.A. affy - analysis of Affymetrix GeneChip data at the probe level. *Bioinformatics* **20**, 307-315 (2004).

42. Wilson, C.L. & Miller, C.J. Simpleaffy: a BioConductor package for Affymetrix Quality Control and data analysis. *Bioinformatics* **21**, 3683-5 (2005).

43. Irizarry, R.A., Wu, Z. & Jaffee, H.A. Comparison of Affymetrix GeneChip expression measures. *Bioinformatics* **22**, 789-94 (2006).

44. Ritchie, M.E. *et al.* limma powers differential expression analyses for RNA-sequencing and microarray studies. *Nucleic Acids Research* **43**(2015).

45. Patro, R., Duggal, G., Love, M.I., Irizarry, R.A. & Kingsford, C. Salmon provides fast and bias-aware quantification of transcript expression. *Nat Methods* **14**, 417-419 (2017).

46. Love, M.I., Huber, W. & Anders, S. Moderated estimation of fold change and dispersion for RNA-seq data with DESeq2. *Genome Biol* **15**, 550 (2014).

47. Raudvere, U. *et al.* g:Profiler: a web server for functional enrichment analysis and conversions of gene

925 lists (2019 update). *Nucleic Acids Res* **47**, W191-W198 (2019).

926 48. Flokova, K. *et al.* UHPLC-MS/MS based target profiling of stress-induced phytohormones.
927 *Phytochemistry* **105**, 147-57 (2014).

928 49. Guhl, K. *et al.* The Effect of Exogenous Nitrate on LCO Signalling, Cytokinin Accumulation, and Nodule
929 Initiation in Medicago truncatula. *Genes (Basel)* **12**(2021).

930 50. Yeats, T.H., Sorek, H., Wemmer, D.E. & Somerville, C.R. Cellulose Deficiency Is Enhanced on Hyper
931 Accumulation of Sucrose by a H+-Coupled Sucrose Symporter. *Plant Physiology* **171**, 110-124 (2016).

932 51. Lionetti, V. *et al.* Overexpression of pectin methylesterase inhibitors in Arabidopsis restricts fungal
933 infection by Botrytis cinerea. *Plant Physiol* **143**, 1871-80 (2007).

934

935

Fig.1

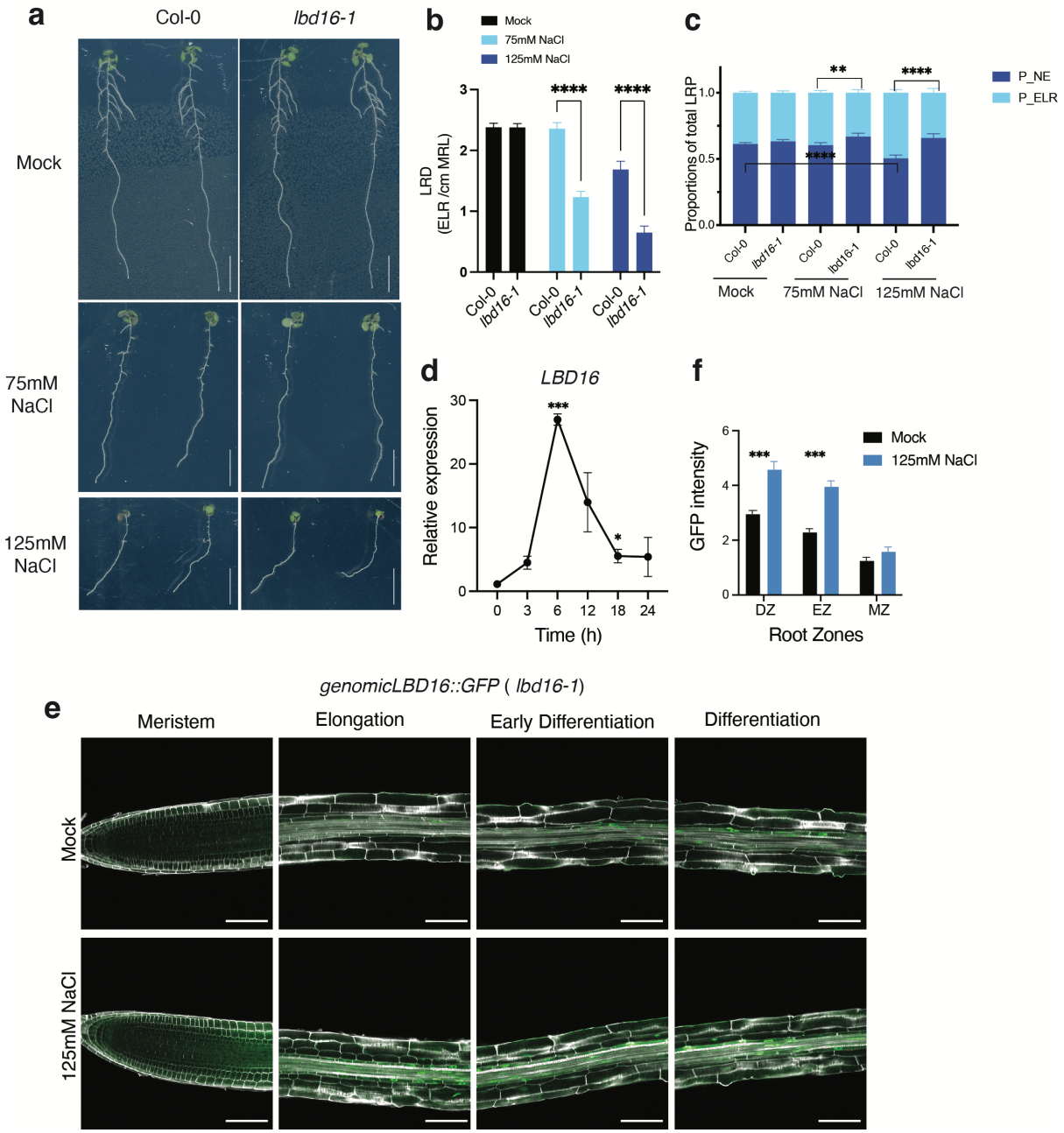
a
Col-0
lbd16-1
Mock
75mM NaCl
125mM NaCl
b
Mock
75mM NaCl
125mM NaCl
LRD (ELR /cm MRL)
****
****
Col-0
lbd16-1
c
Proportions of total LRP
P_NE
P_ELR
**
****
****
Mock
75mM NaCl
125mM NaCl
d
LBD16
Relative expression
***
*
Time (h)
f
GFP intensity
Mock
125mM NaCl
***
***
DZ
EZ
MZ
Root Zones
genomicLBD16::GFP (lbd16-1)
e
Meristem
Elongation
Early Differentiation
Differentiation
Mock
125mM NaCl

936

937

Fig.2

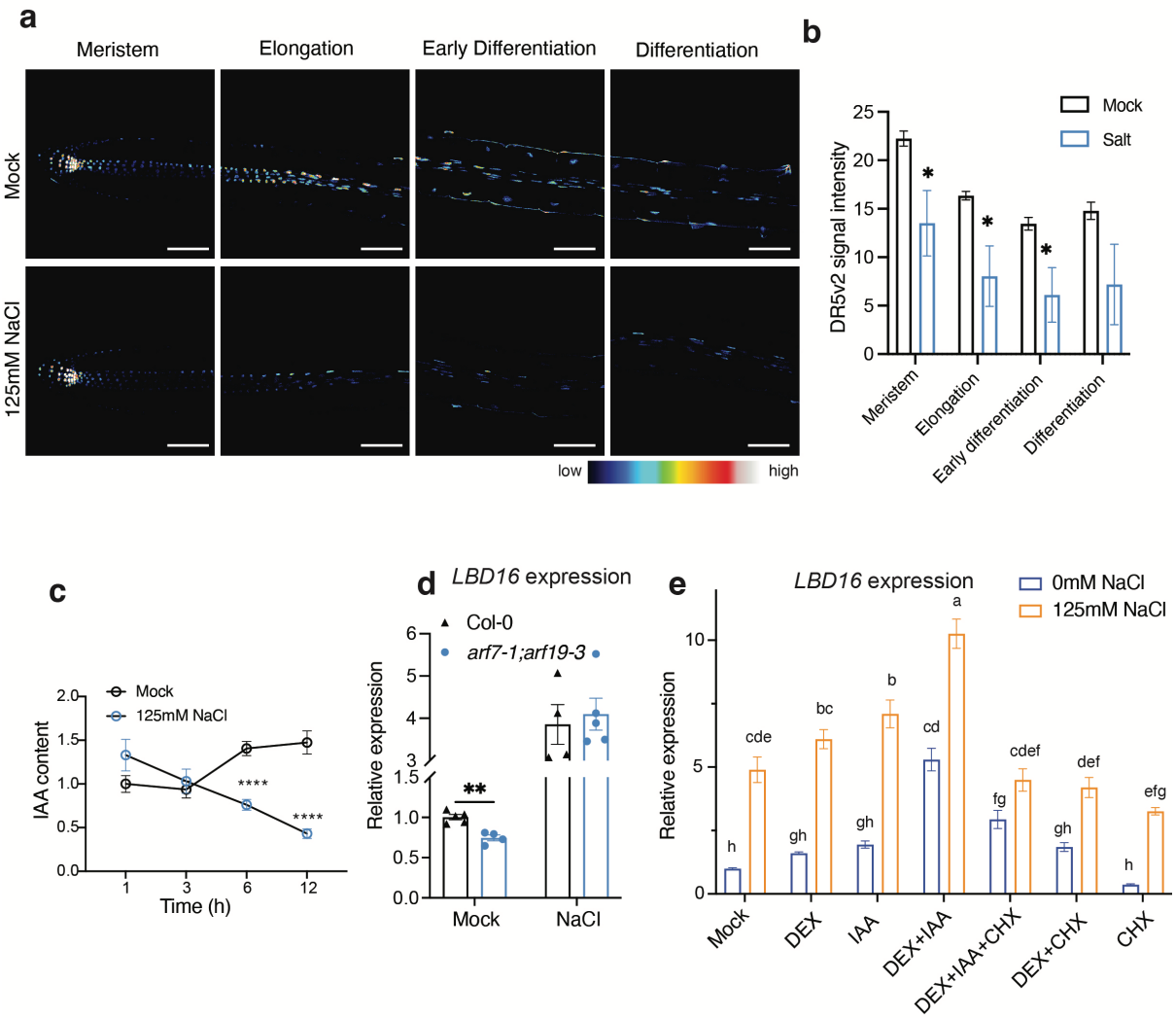
a
Meristem
Elongation
Early Differentiation
Differentiation
Mock
125mM NaCl
low
high
b
Mock
Salt
DR5v2 signal intensity
Meristem
Elongation
Early differentiation
Differentiation
c
Mock
125mM NaCl
IAA content
Time (h)
d
LBD16 expression
Col-0
arf7-1;arf19-3
Relative expression
Mock
NaCl
e
LBD16 expression
0mM NaCl
125mM NaCl
Relative expression
Mock
DEX
IAA
DEX+IAA
DEX+IAA+CHX
DEX+CHX
CHX

938

939

Fig.3

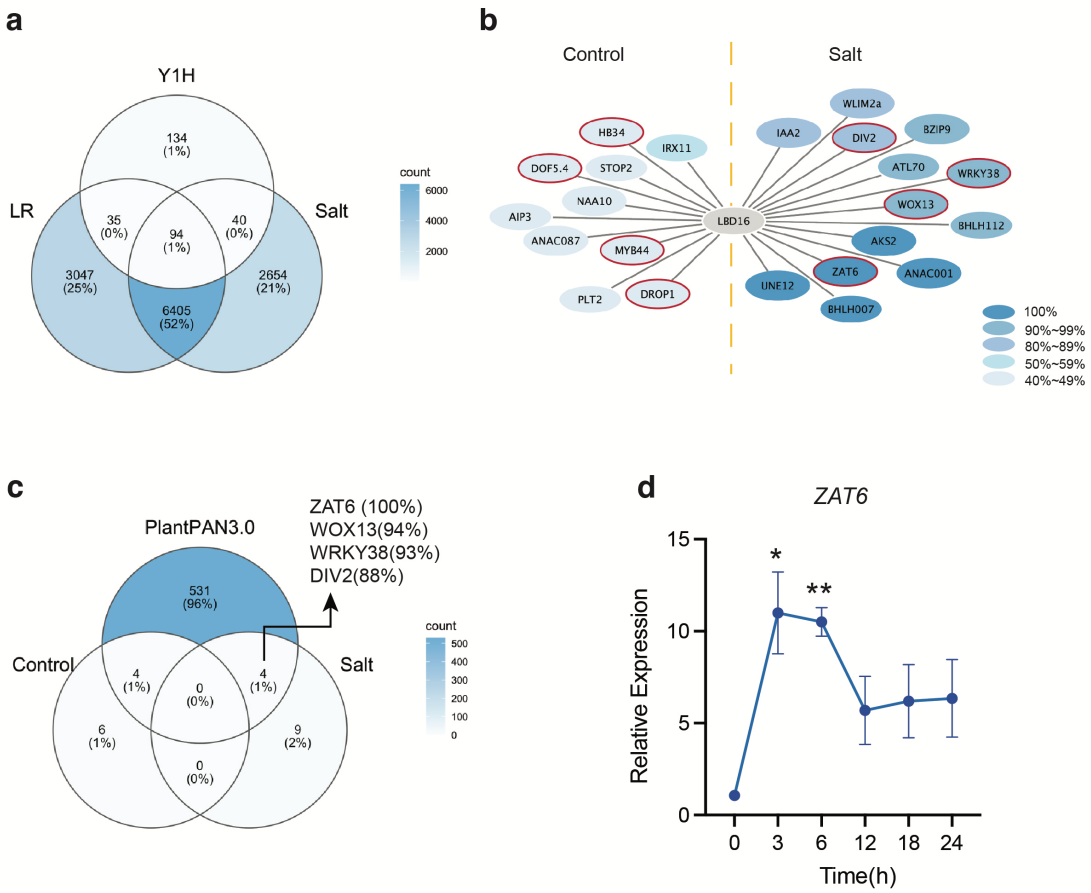
a
Y1H
LR
Salt
134
(1%)
35
(0%)
94
(1%)
40
(0%)
3047
(25%)
6405
(52%)
2654
(21%)
count
6000
4000
2000
b
Control
Salt
HB34
IRX11
DOF5.4
STOP2
NAA10
AIP3
ANAC087
MYB44
PLT2
DROP1
LBD16
WLIM2a
IAA2
DIV2
BZIP9
ATL70
WRKY38
WOX13
BHLH112
AKS2
ZAT6
ANAC001
UNE12
BHLH007
100%
90%~99%
80%~89%
50%~59%
40%~49%
c
PlantPAN3.0
ZAT6 (100%)
WOX13(94%)
WRKY38(93%)
DIV2(88%)
Control
Salt
531
(96%)
4
(1%)
0
(0%)
4
(1%)
6
(1%)
0
(0%)
9
(2%)
count
500
400
300
200
100
0
d
ZAT6
Relative Expression
Time(h)
15
10
5
0
0
3
6
12
18
24
*
**

Fig.4

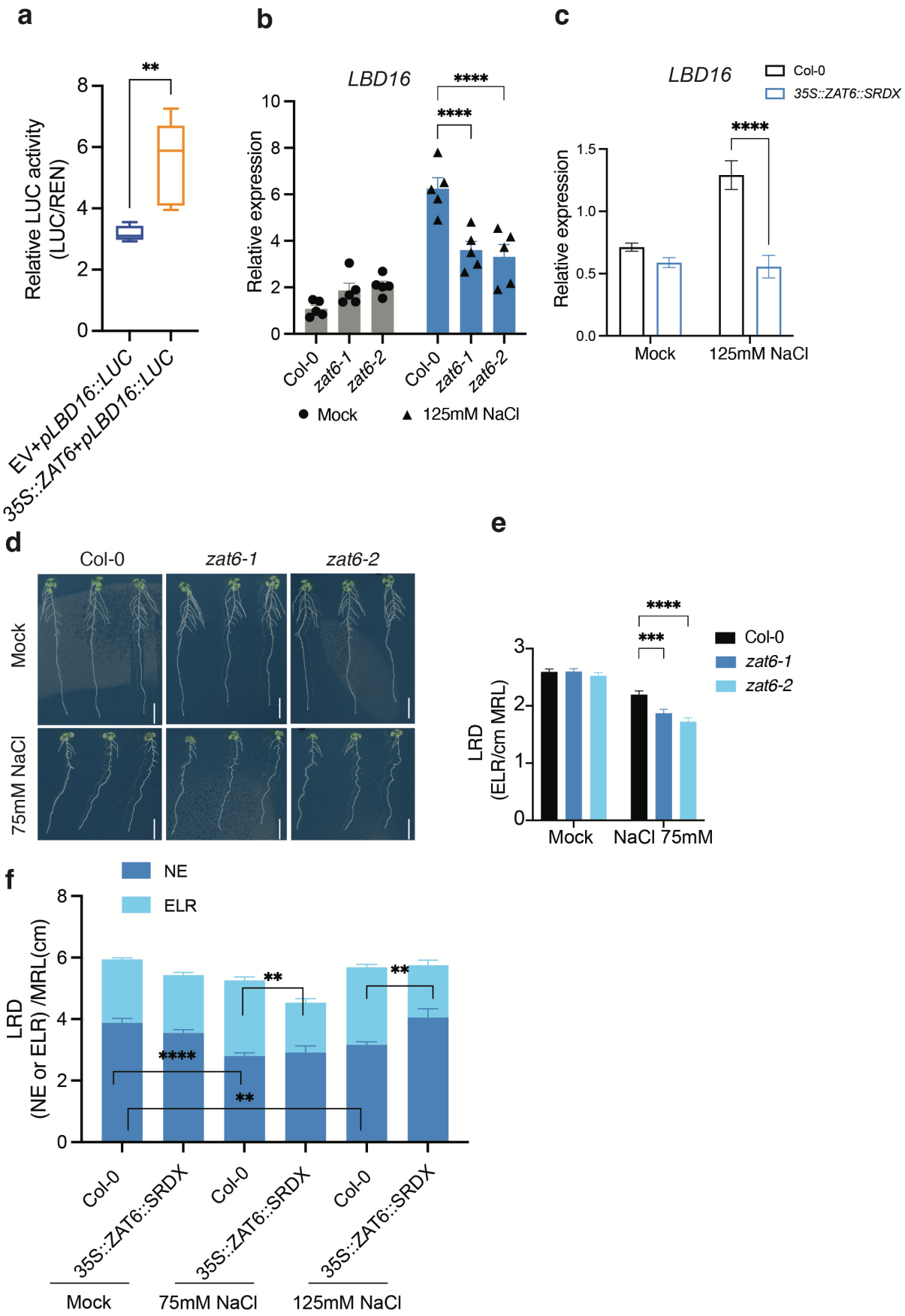
a
Relative LUC activity (LUC/REN)
**
EV+pLBD16::LUC
35S::ZAT6+pLBD16::LUC
b
LBD16
Relative expression
****
****
Col-0
zat6-1
zat6-2
Mock
125mM NaCl
c
LBD16
Col-0
35S::ZAT6::SRDX
Relative expression
****
Mock
125mM NaCl
d
Col-0
zat6-1
zat6-2
Mock
75mM NaCl
e
LRD (ELR/cm MRL)
****
***
Col-0
zat6-1
zat6-2
Mock
NaCl 75mM
f
NE
ELR
LRD (NE or ELR) /MRL(cm)
**
****
**
**
Col-0
35S::ZAT6::SRDX
Mock
75mM NaCl
125mM NaCl

Fig.5

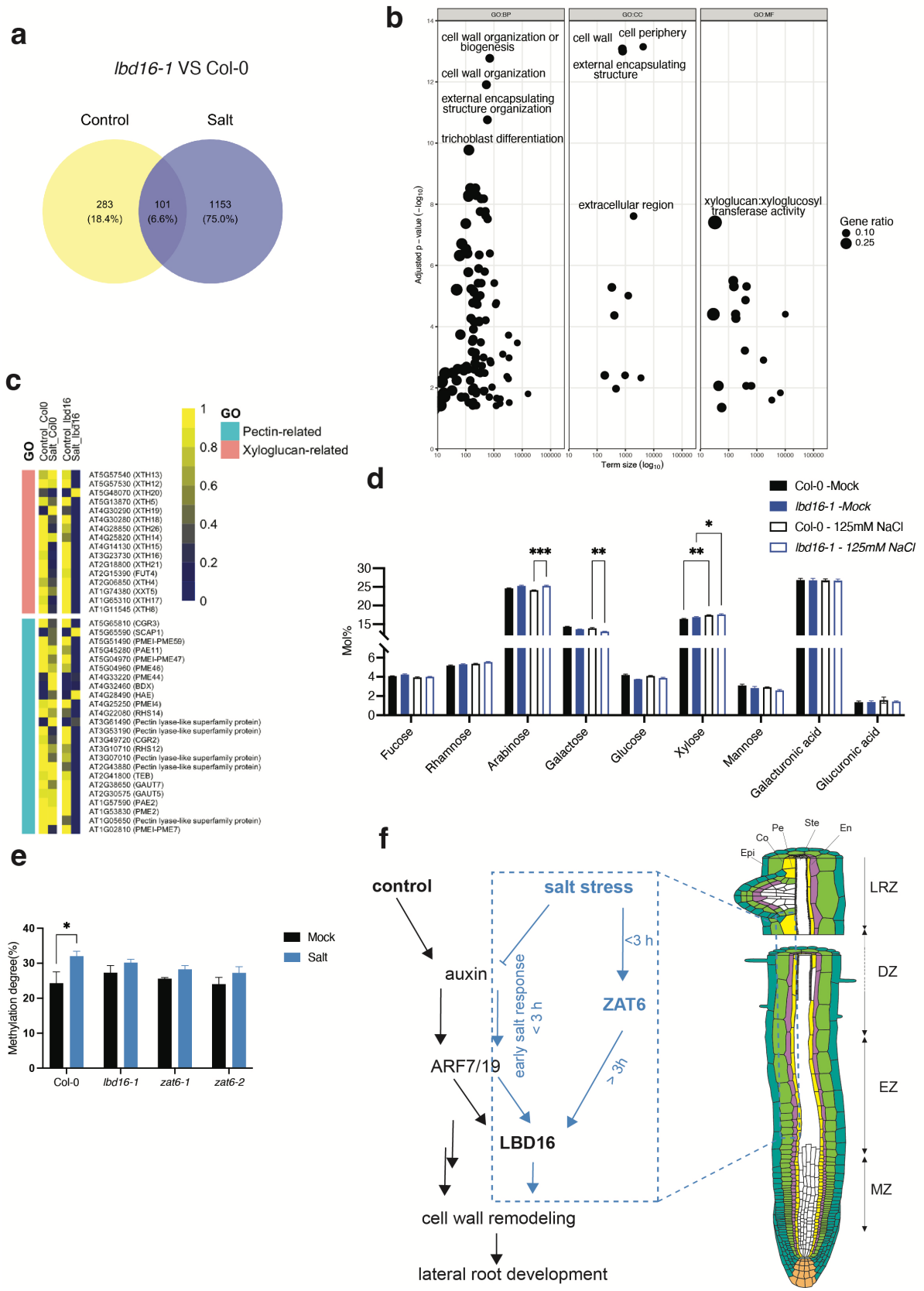
a
lbd16-1 VS Col-0
Control
Salt
283 (18.4%)
101 (6.6%)
1153 (75.0%)
b
GO:BP
GO:CC
GO:MF
cell wall organization or biogenesis
cell wall organization
external encapsulating structure organization
trichoblast differentiation
cell wall
cell periphery
external encapsulating structure
extracellular region
xyloglucan:xyloglucosyl transferase activity
Adjusted p-value (−log10)
Term size (log10)
Gene ratio
0.10
0.25
c
GO
Control_Col0
Salt_Col0
Control_lbd16
Salt_lbd16
Pectin-related
Xyloglucan-related
d
Col-0 -Mock
lbd16-1 -Mock
Col-0 - 125mM NaCl
lbd16-1 - 125mM NaCl
Mol%
Fucose
Rhamnose
Arabinose
Galactose
Glucose
Xylose
Mannose
Galacturonic acid
Glucuronic acid
e
Methylation degree(%)
Mock
Salt
Col-0
lbd16-1
zat6-1
zat6-2
f
control
salt stress
auxin
ARF7/19
early salt response < 3 h
<3 h
ZAT6
> 3h
LBD16
cell wall remodeling
lateral root development
Epi
Co
Pe
Ste
En
LRZ
DZ
EZ
MZ

944